Clays and Clay Minerals, Vol. 35, No. 3, 161–169, 1987.

WEATHERING OF BASALT: CHANGES IN ROCK CHEMISTRY AND MINERALOGY

RICHARD A. EGGLETON, CHRIS FOUDOULIS, AND DANE VARKEVISSER
Department of Geology, Australian National University
Canberra, ACT 2601 Australia

Abstract—The weathering of eastern Australian basalts, sampled from the rounded, hard, core-stone to the rind of softer weathered material, has been examined by bulk chemical analyses, thin section petrography, electron microprobe, and X-ray powder diffraction analyses. Using density as a measure of weathering intensity, data from four core-stones show that at a stage of weathering in which the total loss due to dissolution is ⅓ (i.e., at the core-stone rim), the percentages lost of the following major elements are: Ca, 85; Mg, 80; Na, 70; K, 50–80; P, 55; Si, 45; Mn, 40; Al, 5; Fe, 0; and Ti, 0. With more intense weathering, deposition of some elements, particularly rare earths and Ba, and mobilization and deposition of Al and Fe make quantification impossible. The rate of weathering of individual minerals is consistent with the well-known susceptibility series: glass ~ olivine > plagioclase > pyroxene > opaque minerals. Clay minerals in the core-stones are dominated by smectites, whereas those in the surrounding more intensely weathered rinds are dominated by halloysite and goethite.

Key Words—Basalt, Core-stone, Element mobilization, Goethite, Halloysite, Smectite, Weathering.

INTRODUCTION

The investigations described in this and succeeding papers of this series were conducted to understand the mechanism of basalt weathering by examining the process at the maximum available resolution. Optical microscopic, X-ray powder diffraction, transmission and scanning electron microscopic, bulk chemical, energy-dispersive X-ray, electron microprobe, and various other analytical techniques were used to trace mineral alterations and to evaluate these alterations within a broader framework of the bulk changes occurring in the whole rock during the weathering process.

The present paper describes the larger scale aspects of the weathering of several southeastern Australian basalts on samples taken from the fresh, rounded, core-stone out to the edge of the surrounding coherent weathering rinds and discusses the changes in bulk-rock chemistry and mineralogy that accompanied this early weathering. Later papers will present detailed examinations of the alteration of individual minerals, including the weathering of olivine to iddingsite and bowlingite and the weathering of plagioclase, pyroxene, and opaque oxides.

BACKGROUND

Rock weathering begins when weathering agents first react chemically with the minerals of the rock; however, many weathering studies pass over these initial reactions and concentrate on the formation of saprolites and soils. The minerals in a saprolite that ultimately transform to produce the constituents found in the overlying soil are themselves alteration products of the initial weathering of the minerals of the parent rock. As a prelude to understanding the formation of saprolite zones and soil horizons formed from them, it is vital to understand first the chemical and mineralogical changes that attend these early weathering reactions.

Many of the earlier studies of basalt weathering have been summarized by Loughnan (1969). Volcanic glass is the most susceptible component of such rocks; it alters to palagonite. Almost as susceptible is olivine, which may alter to saponite or nontronite (Craig and Loughnan, 1964), or, after loss of magnesia and oxidation of iron, to hematite, maghemite, or goethite. Basalts in New South Wales studied by Craig and Loughnan (1964) show the mineral susceptibility sequence olivine > pyroxene> plagioclase > sanidine. The ferromagnesian minerals form pseudomorphs of trioctahedral smectite, whereas plagioclase alters to pseudomorphous dioctahedral smectite. Alkali feldspar alters to kaolinite or halloysite.

Colman's (1982) study of the chemical weathering of basalt and andesite core-stones synthesized the broad chemical reactions and mineralogical transformations that take place in early basalt weathering. He found the susceptibility of various minerals to weathering increases generally in the sequence: glass > olivine > pyroxene > amphibole > plagioclase > K-feldspar, but with some variability. Ultimately, all these minerals alter to a mixture of allophane, iron oxide-hydroxide, and clay minerals. Colman also described various stages in the alteration of the basalt and andesite minerals, classifying each product on the basis of its optical appearance, qualitative electron probe analysis, and some X-ray powder diffraction observations. Many of the alteration minerals were described in only rather imprecise terms (e.g., 'iddingsite', chlorophaeite, al-

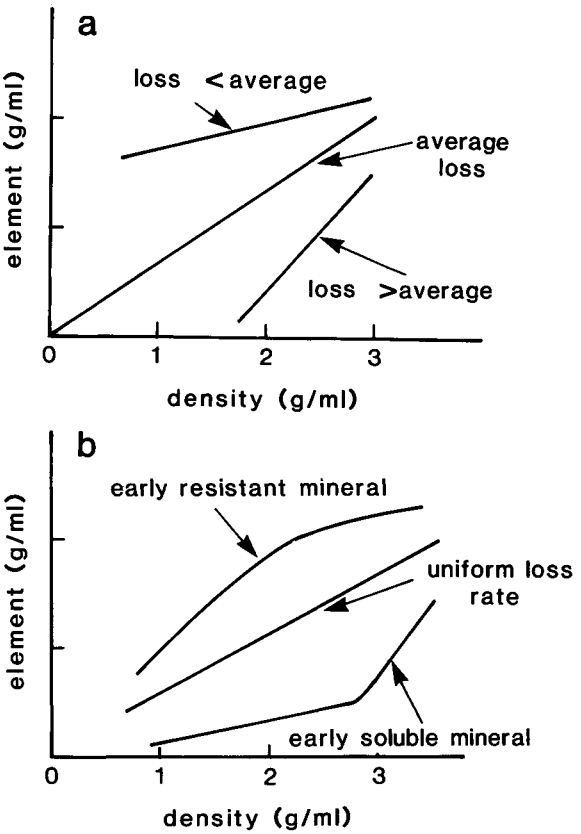

Figure 1. Element or oxide loss in mass/unit volume related to density. (a) General trends shown by an element present in most minerals of the rock (e.g., Si). An element whose loss rate is less than the average (=total) loss rate gives a lower gradient than one whose loss rate is average. (b) Trends shown by an element dominantly in one mineral (e.g., Na, found only in plagioclase). A resistant mineral will give rise to a lower gradient at the start of weathering, which steepens as other more mobile elements are lost.

lophane, iron oxide-hydroxide), but Colman's descriptions provide a valuable basis for further study.

Colman (1982) pointed out several ways of relating chemical movement during weathering, including weathering indexes, standard cell calculations, ratio of elements to an immobile element, and calculations based on constant volume using density measurements (isovolumetric). Density (or specific gravity) gives a measure of the total loss through leaching, provided that no deposition has occurred from outside the core-stone, and neither expansion nor contraction of the rock has taken place. Density is used throughout the present study to convert bulk-rock elemental weight percentages to g/cm^3 of rock, except for a few samples in which specimen incoherence prevented a density measurement. Colman (1982) speculated that a volume loss may accompany rind formation, despite the fact that he reported no thin section evidence for such a loss, because Ti and other less mobile elements increased in concentration, if no volume loss was assumed. On the basis of constant Ti, he calculated a volume loss of 40–50%, consistent with the very large decreases in density reported by Hendricks and Whittig (1968) for andesite weathering.

In a broad sense, weathering intensity increases smoothly from the center of a core-stone outward, but this progression may be interrupted locally by increased weathering on either side of cracks. Density, therefore, provides a more reliable estimate of weathering intensity than distance from a core-stone center or profile depth. Accordingly, density has been used as the ordinate to compare elemental mobility during weathering. Graphs of each element's mass/unit volume vs. whole rock density through a weathering profile can be thought of as showing single element density vs. total element density and thereby allows a quantitative comparison of element loss to be made (Figure 1).

Colman (1982) concluded that for his data elemental gains and losses were best referenced to TiO_2 as an assumed immobile element, an assumption shared by many previous workers. For a few friable samples in the present study, on which density could not be measured, densities were calculated assuming immobile Zr, Ti, and Nb if these three elements correlated closely on a weight percentage basis.

ANALYTICAL METHODS

Bulk chemical analyses of various basalt core-stones and rinds were made for all components except Na, H_2O, CO_2, and Fe(II) by X-ray fluorescence analysis (Norrish and Chappell, 1977). Sodium was determined by flame photometry, H_2O by absorption on P_2O_5, and CO_2 by absorption on NaOH. Elemental analyses of minerals were made by energy-dispersive electron microprobe (N. Ware, analyst) on moderately to well-polished mineral grains. Density was measured by water displacement using a top-loading balance. Absorbant samples (almost all) were coated with paraffin wax after weighing in air, and the volume measured by water displacement was corrected by subtraction of the paraffin wax volume estimated by weight. Clay minerals were identified by standard X-ray powder diffraction methods using a Philips P.W.1540 goniometer and Co radiation.

RESULTS AND INTERPRETATION

The Baynton basalt

Description. Nine samples (B1–B9) were cut from a continuous but cracked 90-mm section of a core-stone and rind collected from a small road cut near Baynton, Victoria, Australia. This outcrop of the Newer Volcanics of the Victorian Tertiary basalts was studied by Wilson (1978). Fresh basalt occurs at this site (Wilson's sample 2-0), although the freshest sample of the present

https://doi.org/10.1346/CCMN.1987.0350301 Published online by Cambridge University Press

study (B1) has iddingsite rims on the olivine. The rock is a tholeiitic basalt, containing olivine (11%), clinopyroxene (10%), orthopyroxene (5%), plagioclase (39%), and glass (30%). Contained in the glass are ilmenite needles, titanomagnetite, and apatite.

Chemistry. Selected elemental contents for the Baynton samples (Table 1) are plotted in Figure 2 as g/cm^3 of oxide for major elements, or as g/1000 cm^3 for trace elements. Al and Fe are clearly immobile during the weathering of this core stone as are Ti, Zr, and Nb (not plotted). The other elements show a uniform depletion, except for Ca and Na, for which there is evidence that the gradient increases towards the outer part of the rind, and K, Rb, and Mg, which show a rapid early loss. Only Ba shows a clear increase in mass/unit volume with increased weathering (see Table 1, which shows that the more weathered samples B7, B8, and B9 contain as much as twice as much Ba as sample B1).

The major element trends are readily explained in terms of the susceptibility of the constituent minerals to weathering. The glass weathers most readily, releasing K, Na, and Si, and the residual elements Al, Fe, and Ti concentrate in its alteration product. The glass is the only source of K in this basalt; hence, K is depleted early in weathering, together with the geochemically similar Rb. Average analyses of glass and its weathered product (Table 2) show a sharp drop in alkalis outward coinciding with a marked increase in Fe and Ti. SiO_2 in weathered glass falls to almost half its original value, and Al_2O_3 increases by about 30%. Olivine weathers as early as the glass, forming Si-Mg-depleted, Fe-enriched iddingsite rims. The iddingsite rims become more iron-rich and Si-Mg-poor as weathering proceeds. Plagioclase shows no noticeable alteration until sample B4; this slow start in weathering is reflected in the initial flatter trend of the CaO and Na_2O graphs (Figures 2f and 2g). Sr, which is normally incorporated in plagioclase (Henderson, 1982), shows a similar trend. Pyroxene was also found to be unaltered in the first three Baynton samples. In samples B4–B9 pyroxene is altered to an iddingsite-like product, with losses of Mg, Ca, and Si.

The preceding general interpretation of the chemical results was tested for consistency using modal analyses and mineral compositions to calculate bulk chemistry at various stages in the alteration. Table 3 lists the whole-rock analysis for sample B7 and the predicted composition calculated from mineral data. The agreement between the actual and predicted bulk composition supports the interpretation of the major element variation on the basis of mineral alteration, in that it provides a quantitative check of the internal consistency of the measurements.

The uniform slope of most of the element-loss curves for the Baynton samples allows a quantitative estimate of the difference in loss of the basalt elements. The graphs relate the loss of an individual element to the overall loss, summarized in Table 4 as percentage loss of the element at a 33% density decrease. This value was chosen because it intercepts the straight line portion of all graphs and occurs in the outermost weathering rind of the basalt core-stones studied here. At the stage where its density has fallen by one third, the weathered Baynton basalt contains 8 wt. % water.

Carool basalt

Petrography. Samples of basalt from the Tertiary Lamington Volcanics were collected near Carool, northern New South Wales, Australia, in a recent road cut (Figure 3). The samples were collected over a 140-mm interval from fresh core-stone to rind, and include more highly weathered material than the Baynton sequence. Samples C1–C4 are from an uncracked core-stone; samples C5–C7 are from concentrically cracked and color-banded rock rimming the core-stone.

The fresh basalt contains plagioclase (Ab_{50}) phenocrysts as long as 5 mm, smaller olivine (Fo_{65}) grains, and equant augite and orthopyroxene, surrounded by glass containing numerous ilmenite needles and acicular clinopyroxene. Early alteration has changed the glass to yellow palagonite and the olivine to brown iddingsite and bowlingite. Such alteration is evident over a distance of about 20 mm, and is followed by a sharp change to more obviously weathered rock marked by a 5-mm-thick, orange-colored rind. The color change is largely caused by a change in the color of the palagonite from yellow to orange-red and by the complete replacement of olivine and pyroxene by a dark-red, isotropic alteration product, predominantly goethite. In this zone the feldspar has begun to alter, as evidenced by a decrease in its birefringence, the presence of smectite lines in XRD photographs of the feldspar alteration pseudomorph, and a large increase in the intensity of the smectite XRD peak from the whole rock samples. Halloysite is also present in small amounts.

In the outer part of the Carool core-stone (samples C5–C7) concentric cracks are filled with halloysite. Thin section examination indicates that this part of the core-stone has fractured and expanded by about 15%. The altered basalt fragments between the cracks are composed of smectite, halloysite, goethite, and remnant plagioclase.

Chemistry. The elements Ti, Zr, and Nb, which are immobile in the Baynton basalt samples, are also immobile in the coherent core-stone and rind samples C1–C4. In the expanded samples C5–C7 the ratio between these elements is constant, whereas on the basis of measured density, the mass/unit volume of these elements decreases. Correcting the measured density

Table 1. Chemical analyses of basalt core-stones, southeastern Australia.[1]

	M10	M11	M12	M13	M15	M17	M19	M20	M21	M22	M23	M24	M25	C1	C2
(Wt. %)															
SiO_2	47.11	32.61	37.42	45.01	36.70	36.33	46.50	46.30	46.84	46.47	42.27	43.84	42.82	50.85	50.88
TiO_2	1.61	1.96	2.03	1.85	2.89	3.21	1.78	1.75	1.79	1.77	1.79	1.75	1.68	2.43	2.49
Al_2O_3	14.69	17.34	17.58	16.65	24.16	26.46	14.87	14.70	15.00	14.99	15.20	14.84	17.15	15.14	15.56
Fe_2O_3	2.95	20.31	17.00	11.65	15.77	14.64	3.88	3.32	6.57	7.08	13.02	10.89	11.90	2.42	2.79
FeO	7.53	3.51	2.60	1.78	0.82	0.99	7.34	7.77	4.88	4.55	0.82	1.48	0.37	8.00	7.12
MnO	0.17	0.19	0.14	0.17	0.12	0.08	0.15	0.16	0.15	0.15	0.15	0.19	0.11	0.14	0.17
MgO	9.45	3.96	3.89	4.31	1.27	0.87	8.93	9.30	7.90	7.82	4.72	5.84	3.57	3.81	2.91
CaO	8.13	1.45	1.50	4.60	0.67	0.53	8.57	8.51	8.59	8.55	2.91	5.00	1.71	7.04	7.24
Na_2O	2.72	0.44	0.85	1.94	0.07	0.07	2.62	2.56	2.62	2.66	1.09	1.58	0.60	3.69	3.80
K_2O	0.96	0.53	0.82	1.03	0.02	0.01	0.90	0.88	0.81	0.87	0.73	0.71	0.63	1.89	1.93
P_2O_5	0.34	1.21	0.49	0.39	0.24	0.12	0.42	0.41	0.42	0.42	0.43	0.39	0.38	0.83	0.86
H_2O+	2.20	9.20	7.80	5.34	10.47	11.19	2.65	2.73	2.63	2.80	6.85	5.46	7.85	1.06	1.09
H_2O-	1.24	7.57	8.01	5.12	6.89	5.69	1.22	1.22	2.31	2.35	9.58	8.13	12.09	1.52	1.42
CO_2	0.38	0.09	0.11	0.01	0.13	0.17	0.10	0.09	0.09	0.08	0.14	0.11	0.17	0.90	1.61
Total	99.48	100.37	100.24	99.85	100.22	100.36	99.93	99.70	100.60	100.56	99.70	100.21	101.03	99.72	99.87
(ppm)															
Ba	245	1160	480	565	165	230								600	620
Rb	21	13	19	25	1	0								35	34
Sr	397	1070	234	297	110	81								551	573
Pb	4	5	4	5	5									4	5
Zr	153	179	—	174	265	279								314	326
Nb	40	48	—	46	73	81								24	25
Y	21	38	35	40	36	11								28	31
La	22	69	26	31	88	15								31	34
Ce	49	54	45	62	100	78								76	81
V	151	232	204	148	259	254								113	111
Cr	256	331	342	288	615	496								47	49
Ni	181	354	387	255	358	491								66	65
Cu	53	—	—	—	—	139								23	23
Zn	94	235	191	113	136	162								138	148
S.G.	2.83	2.34	2.24	2.46	1.56	1.41								2.71	2.72

Table 1. Continued.

	C3	C4	C5	C6	C7	B1	B2	B3	B4	B5	B6	B7	B8	B9
(Wt. %)														
SiO_2	51.20	44.68	42.92	44.10	41.29	52.17	52.46	51.88	48.24	46.89	47.99	45.37	42.70	46.85
TiO_2	2.73	3.25	3.28	3.32	3.11	1.93	1.95	2.04	2.21	2.34	2.28	2.39	2.76	2.44
Al_2O_3	16.86	16.57	20.08	20.47	21.16	14.44	14.53	14.98	16.49	17.50	17.02	19.94	19.02	18.40
Fe_2O_3	6.89	12.74	13.10	11.75	12.87	5.67	5.85	6.69	9.72	10.85	10.33	11.18	13.47	12.62
FeO	2.96	2.61	1.67	1.55	1.46	5.03	4.97	4.51	2.86	2.47	2.61	2.67	2.32	1.37
MnO	0.07	0.06	0.16	0.18	0.19	0.12	0.11	0.12	0.10	0.10	0.11	0.11	0.12	0.09
MgO	1.28	1.18	0.75	0.70	0.74	5.87	5.83	5.50	4.88	4.75	4.73	5.12	4.76	3.70
CaO	6.23	4.17	0.40	0.26	0.21	7.60	7.56	7.74	7.06	5.90	6.58	5.24	3.35	4.79
Na_2O	3.68	2.66	1.55	1.37	0.99	3.00	2.98	3.01	2.97	2.65	2.87	2.23	1.49	2.65
K_2O	1.80	1.52	1.73	1.89	1.35	1.19	1.14	0.97	0.48	0.43	0.48	0.43	0.41	0.48
P_2O_5	0.95	1.11	0.57	0.49	0.63	0.32	0.30	0.31	0.30	0.30	0.30	0.30	0.21	0.28
H_2O+	2.13	4.25	7.30	7.35	8.09	1.10	1.08	1.21	2.22	3.46	2.70	4.37	6.29	3.95
H_2O-	2.43	4.43	6.63	6.56	7.40	0.62	0.77	0.84	1.92	2.13	1.94	2.08	2.92	3.18
CO_2	0.44	0.81	0.33	0.33	0.38	0.36	0.11	0.08	0.13	0.23	0.20	0.36	0.68	0.14
Total	99.65	100.04	100.47	100.32	99.87	99.42	99.64	99.88	99.58	100.00	100.14	101.79	100.50	100.94
(ppm)														
Ba	715	970	775	660	615	245	255	270	300	445	355	555	745	410
Rb	27	15	22	28	17	36	34	27	5	4	4	5	5	5
Sr	570	33	89	84	85	346	355	364	382	342	377	285	208	352
Pb	5	7	5	6	6	5	4	4	5	5	6	4	6	6
Zr	356	409	421	434	412	189	193	199	217	233	226	237	275	–
Nb	27	32	33	34	33	23	23	24	26	28	27	28	32	–
Y	35	33	44	61	189	29	29	27	25	22	25	18	11	19
La	38	34	33	70	231	35	37	26	30	28	32	22	13	25
Ce	92	84	112	183	401	50	51	46	45	45	47	38	21	36
V	126	153	152	162	158	147	149	159	155	165	155	180	192	137
Cr	54	65	68	70	66	253	257	252	265	286	272	298	342	326
Ni	28	38	82	76	47	132	135	124	138	153	145	189	240	–
Cu	31	26	29	30	25	52	54	53	52	54	53	56	64	60
Zn	164	183	212	185	121	134	135	140	147	151	147	157	162	–
S.G.	2.50	2.13	1.79	1.72	1.56	2.62	2.59	2.55	2.31	2.14	2.25	2.10	1.83	2.06

[1] B. W. Chappell, analyst; H_2O- = wt. % water evolved <110°C; H_2O+ = wt. % water evolved >110°C; S.G. = specific gravity. Samples M10–M25 = Monaro basalt; samples B1–B9 = Baynton basalt; samples C1–C7 = Carool basalt.

Table 2. Electron microprobe analyses of Baynton basalt samples B1 and B7.

	Fresh minerals (B1)							Altered minerals (B7)		
	Glass	Olivine	Clino-pyrox-ene	Ortho-pyrox-ene	Plagio-clase	Spinel	Ilmenite	Glass	Olivine	Plagio-clase
(Wt. %)										
SiO_2	62.10	38.50	51.80	54.29	54.31	0.00	0.00	36.30	28.75	38.70
TiO_2	2.10	0.00	0.64	0.24	0.00	27.40	52.14	3.40	0.36	0.18
Al_2O_3	13.60	0.17	2.48	1.89	28.83	0.00	0.00	20.10	2.00	32.00
Fe_2O_3	1.60	0.00	0.00	0.00	0.00	20.90	0.00	17.10	40.86	5.40
FeO	5.00	22.50	9.10	12.32	0.82	51.70	46.20	0.00	0.00	0.00
MnO	0.00	0.22	0.19	0.12	0.00	0.00	0.50	0.00	0.20	0.00
MgO	0.40	39.20	16.33	28.58	0.00	0.00	1.10	0.70	21.16	0.00
CaO	2.90	0.21	18.48	1.85	11.77	0.00	0.00	1.40	0.29	0.17
K_2O	3.40	0.00	0.00	0.00	0.33	0.00	0.00	0.20	0.00	0.21
Na_2O	4.40	0.00	0.32	0.00	4.62	0.00	0.00	0.10	0.00	0.14
Total	95.70	100.80	99.34	99.28	100.78	100.00	98.84	79.30	93.62	76.80

for the measured expansion brings the Ti, Zr, Nb, Al, and Fe content of samples C5 and C6 close to that of samples C1–C4, whereas sample C7 shows a mass loss. The constancy of these elements suggests that at the centimeter scale they are relatively immobile, although the presence of halloysite-filled cracks is clear evidence for Al (and Si) mobility at least at the hand-specimen scale. Figure 2 shows the relative loss of various elements from the Carool core-stones; SiO_2, CaO, and Na_2O all show roughly linear trends, reflecting the

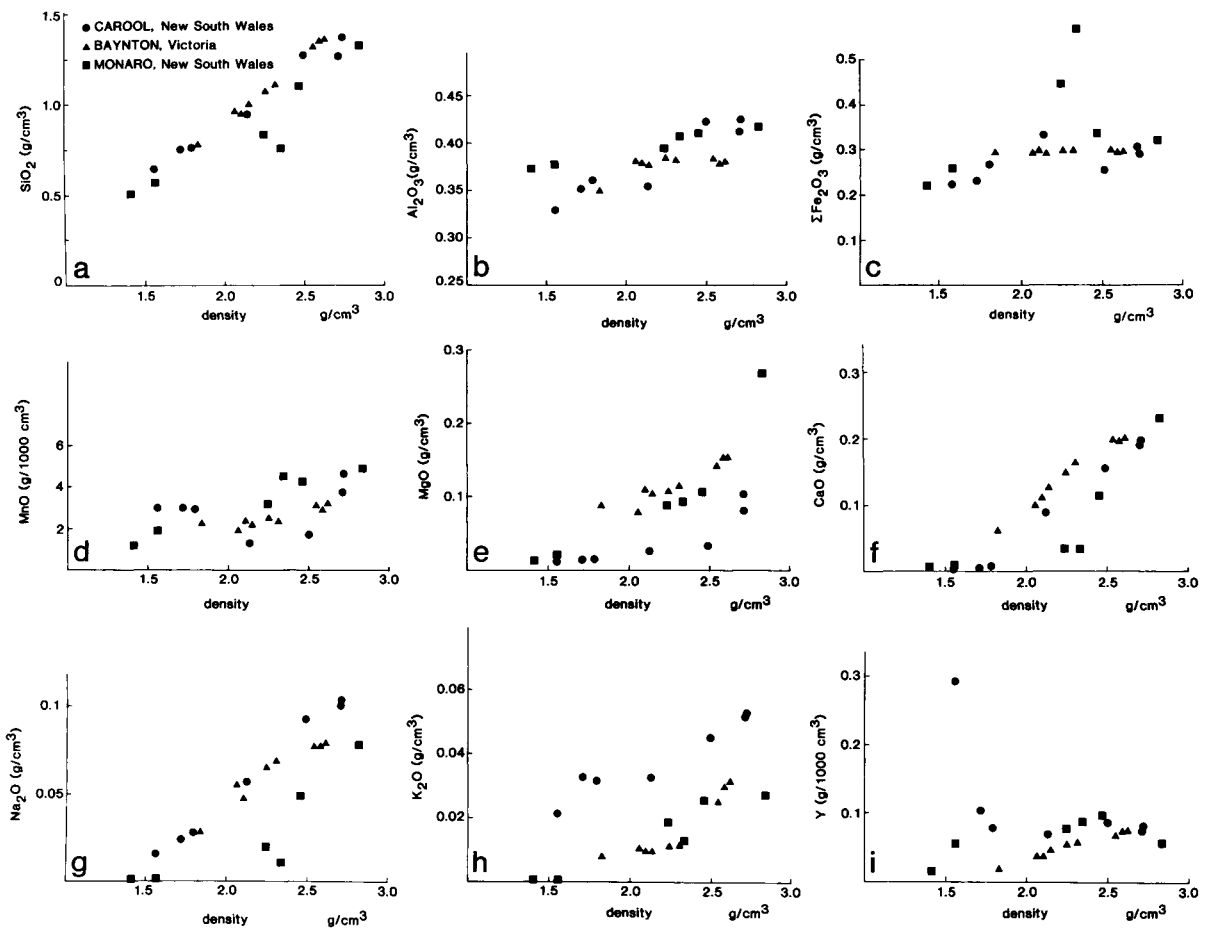

Figure 2. Individual element or oxide vs. density of whole rock. Symbols as in (a).

https://doi.org/10.1346/CCMN.1987.0350301 Published online by Cambridge University Press

Table 3. Mode and comparison between estimated[1] and measured rock composition of weathered basalt sample B7 from Baynton, Victoria.

	Mode			Composition	
	(vol. %)	(wt. %)		Estimated (wt. %)	Measured (wt. %)
Glass	12.00	12.96	SiO_2	44.4	45.40
Olivine	0.50	0.71	TiO_2	2.30	2.40
Clinopyroxene	9.00	12.45	Al_2O_3	17.40	17.90
Orthopyroxene	2.30	3.38	Fe_2O_3	9.30	11.20
Plagioclase	18.30	21.35	FeO	4.20	2.70
Spinel	1.10	2.28	MnO	0.01	0.01
Ilmenite	0.50	1.08	MgO	5.80	5.10
Palagonite (altered glass)	22.20	18.71	CaO	5.60	5.20
Iddingsite	10.60	11.09	K_2O	0.60	0.40
Pclay[2]	18.50	15.99	Na_2O	1.60	2.20
Void	4.90	0.00	H_2O	8.90	9.20
Total	99.90	100.00	Total	100.00	101.71

[1] Estimated composition calculated from mode and mineral compositions listed in Table 2.
[2] Pclay = alteration product of plagioclase.

weathering of plagioclase, the major constituent of this basalt. Figure 2e shows that Mg was rapidly leached, falling to less than half its original content in sample C3. This early loss occurred because Mg is largely concentrated in readily weathered minerals. The rare earth elements Y (Figure 1c) and Ce increase markedly towards the outer parts of the core-stone. Rare-earth phosphates are common minerals in soils (Norrish, 1968), and the increase in rare earth elements in core-stone rinds may reflect their precipitation as phosphates. Banfield (1985) reported such a process for granite weathering. After removal of silicates from sample C7 by digestion in 20% HF for 2 min, XRD patterns showed ilmenite, rhabdophane ($(Ce,La)PO_4 \cdot H_2O$), and the five strongest lines of gorceixite.

Monaro basalts

The alkaline basalts of the Monaro region of southern New South Wales were described by Kesson (1973) and more recently by Jones and Veevers (1982). In the present study, fresh and weathered samples were collected from two localities near Cooma, New South Wales. Their mineralogies are similar; olivine (Fo_{80}), titanaugite, plagioclase (An_{35}), ilmenite, and magnetite.

The basalts M10–M17 were sampled from a core-stone through successive rinds to a deeply weathered saprolite composed chiefly of kaolin and halloysite (Figure 4). The extensive weathering of this sequence has produced macroscopic voids in samples M11–M13, making density measurement unreliable. The ratios among the elements Ti, Zr, and Nb are the same for these three samples, apparently reflecting the immobility of these elements. Relative element loss has been estimated on this basis (i.e., constant Ti, Zr, Nb).

Samples M19–M25 are from a basalt flow having a vesicular top. The more intensely weathered parts of this flow were sampled from the vesicular region; hence, their densities are not comparable to those of the massive unweathered samples. Data from the sequence are included in Table 1, but not in Figure 2.

Petrography. Alteration of the Monaro basalts apparently began with the formation of bowlingite in cracks in the olivine. Green bowlingite is almost ubiquitous in the Monaro basalts; many flows were probably altered during final cooling. Thin section examination clearly shows that recent weathering first enlarged the

Table 4. Element loss (% of original amount) at one-third density decrease (33% total mass loss).

	Baynton	Monaro	Carool
Ca	80	90	90
Mg	60	80	85
Na	65	75	70
K	80	65	50
P	50	55	60
Si	45	45	40
Mn	40	45	v[1]
Al	0	5	10
Fe	0	0	0
Ti	0	0	0
Y	80	0	0
Ce	70	v	5
La	80	v	30
Ba	−85	v	25
Rb	90	70	
Sr	80	~90	90
Cu	25	—	30
Zn	15	v	15
Cr	0	0	0
Nb	0	0	0
Zr	0	0	0
V	10	0	0
Ni	0	0	v

[1] v = variable.

https://doi.org/10.1346/CCMN.1987.0350301 Published online by Cambridge University Press

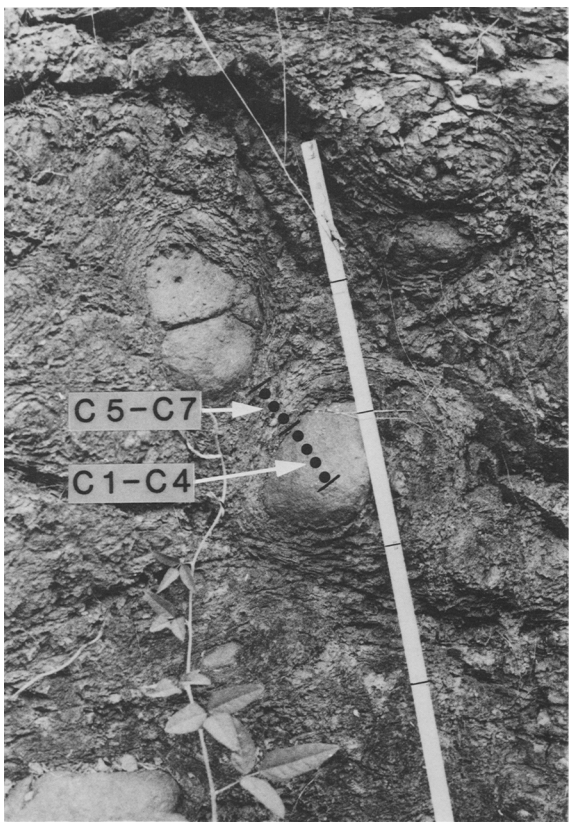

Figure 3. Sample site near Carool, New South Wales. Numbers refer approximately to analysis numbers for samples C1–C7. Scale marks are at 30-cm intervals.

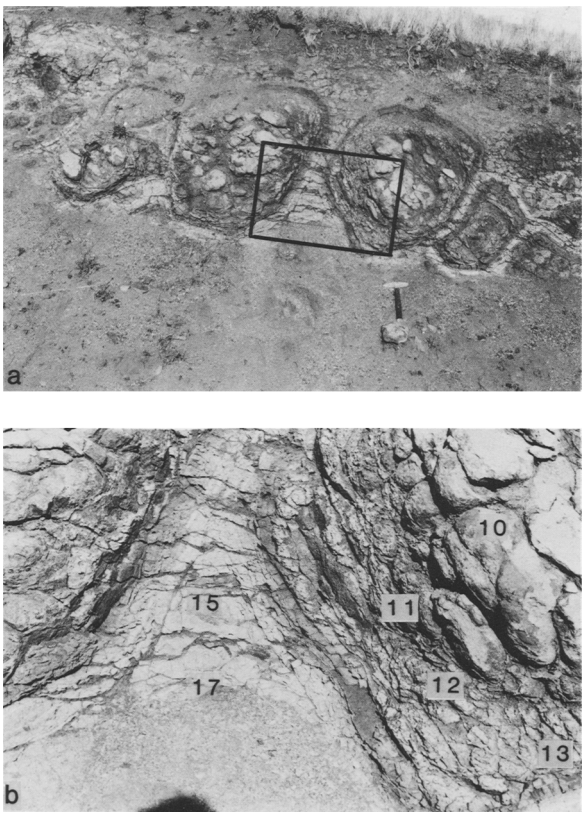

Figure 4. Sample site for Monaro sequence, samples M10–M17. (a) General view of core-stones; box shows area of (b). (b) Detail of sampled core-stone.

areas of bowlingite, and then, as the conditions became oxidizing, the bowlingite and the remaining olivine altered to iddingsite.

Titanaugite is the most resistant silicate in the Monaro basalts; it shows no alteration in samples unless the olivine has almost completely altered to iddingsite. Augite apparently began to alter along cracks where it formed iddingsite, which ultimately replaced the crystal without forming a euhedral pseudomorph. In contrast to olivine, which altered to euhedral, deep-orange pseudomorphs of iddingsite, the pyroxene iddingsite shows a less definite pseudomorph shape and is a paler orange mass.

Plagioclase weathered initially along fractures and cleavage planes, showing the introduction of iron along these surfaces by a yellow discoloration. The resulting feldspar fragments were gradually replaced peripherally by very fine grained, weakly birefringent yellow material, which is pseudomorphous after the original crystal. XRD and electron probe analyses show that at this stage of weathering the alteration assemblage was dominated by smectite. On further alteration, the pseudomorphs after olivine and feldspar remain recognizable, but gradually change appearance. Iddingsite pseudomorphs after olivine develop a rim of isotropic orange-brown material having oriented cleavage traces and a core of similarly randomly oriented, colored isotropic material. A zone of darker brown, more opaque material separates the rim from the core.

The outlines of the feldspar pseudomorphs are less distinct than those of the olivine. The final feldspar alteration product is a colorless to yellow-brown isotropic mass, dominated by halloysite with lesser goethite. XRD data for the alteration sequence represented by samples M11–M17 show that, as for the Carool sequence, the clay mineral assemblage changes from smectite-dominated in the early stages of weathering (samples M11–M13, coherent core-stone) to kaolin-halloysite-dominated in the later stages (samples M15 and M17).

Chemistry. The general chemical trends of the other two profiles are also shown by the Monaro samples, although less clearly. The interpretations that can be placed on them are further limited by the assumption of constant Ti used for samples M11–M13. Approximate values for the element loss at ⅓ total mass loss are included in Table 4 for samples M10–M17. For samples M19 to M25, the relative mobility on a wt. % basis is Ca > Na > Mg > K = Mn > Si > Fe = Ti > Al.

https://doi.org/10.1346/CCMN.1987.0350301 Published online by Cambridge University Press

DISCUSSION AND CONCLUSIONS

During weathering of these three basalts, Ca, Mg, K, Na, Rb, and Sr generally show a rapid, early loss which can be correlated with the alteration of volcanic glass to smectite, the formation of iddingsite, and the early weathering of plagioclase. Si, Mn, P, Cu, and Zn appear to be more slowly and uniformly leached, whereas Ti, V, Cr, Fe, Ni, Zr, and Nb are essentially immobile within coherent core-stones. Al shows a slight loss in the outer parts of the core-stones. The rare earth elements and Ba are lost initially, but appear to be slightly concentrated in the outer rind. Although the climate is somewhat different in the areas studied, the rocks examined at each locality are in near-surface positions (alternately wet and dry), and no obvious relation between climate and relative rate of loss of the elements has been noted, suggesting that the *mechanism* of core-stone weathering has not been affected by climate, although the overall *rate* of weathering may have differed. Claridge and Campbell (1984) reached the same conclusion in their study of dolerite weathering in Antarctica.

These results do not show clearly if any elements were immobile during the more intense weathering that followed exfoliation of the core-stones. In the later stages of saprolite formation, elements leached from the core-stone rinds, or from elsewhere in the profile, may have accumulated in the porous weathered samples (e.g., in the late halloysite veins at Carool). Once this has happened bulk chemical data are impossible to interpret in terms of element movement without an associated, detailed, mineral alteration study. This is because, for example, a bulk analysis indicating 75% loss of an element may be of a sample which had earlier lost 90% of that element and subsequently became enriched. The results presented here indicate that for the major elements, re-enrichment is not significant within the core-stone, but that it is significant for some trace elements (e.g., Y, Ce at Carool).

The constituent minerals of these basalts show the following pattern of weathering susceptibility: glass ~ olivine > plagioclase > pyroxene > opaque minerals. In sample B7, for example, only 5% of the original olivine, 30% of the glass, and 50% of the plagioclase are left, whereas pyroxene and opaque oxides are still essentially unaltered. Thin section examination shows that olivine and glass began to alter at about the same time, but that some glass remained even when the olivine had completely altered to iddingsite. This difference may simply be because more glass was present initially than olivine, or because isolated pockets of glass are preserved in 'cages' of more resistant feldspar.

The order of plagioclase and pyroxene susceptibility found in this work is the reverse of that commonly described (see, e.g., Loughnan, 1969). Although plagioclase began to alter earlier than pyroxene, once started, pyroxene weathered relatively quickly, and was completely altered before plagioclase. Consequently, plagioclase may persist longer than pyroxene, even though it started to weather earlier.

ACKNOWLEDGMENTS

We gratefully acknowledge the support of Australian Research Grant Scheme grant E 8115611R. All chemical analyses were made under the supervision of B. W. Chappell, assisted by R. S. Freeman, E. Webber, and J. Wasik. We also thank G. Taylor and K. L. Smith for stimulating discussion and S. Colman for constructive criticism of the manuscripts.

REFERENCES

Banfield, J. F. (1985) Mineralogy and chemistry of granite weathering: M.Sc. thesis, Australian National University, Canberra, Australia, 229 pp.

Claridge, G. G. C. and Campbell, I. B. (1984) Mineral transformation during the weathering of dolerite under cold arid conditions in Antarctica: *New Zealand J. Geophys.* **27,** 537–546.

Colman, S. M. (1982) Chemical weathering of basalts and andesites: Evidence from weathering rinds: *U.S. Geol. Surv. Prof. Pap.* **1246,** 51 pp.

Craig, D. C. and Loughnan, F. C. (1964) Chemical and mineralogical transformations accompanying the weathering of basic volcanic rocks from New South Wales: *Australian J. Soil Res.* **2,** 218–234.

Henderson, P. (1982) *Inorganic Geochemistry:* Pergamon Press, New York, 353 pp.

Hendricks, D. M. and Whittig, L. D. (1968) Andesite weathering, Part II. Geochemical changes from andesite to saprolite: *Soil Sci.* **19,** 147–153.

Jones, J. G. and Veevers, J. J. (1982) A Cainozoic history of Australia's Southeast Highlands: *Geol. Soc. Aust.* **29,** 1–14.

Kesson, S. E. (1973) The primary geochemistry of the Monaro alkaline volcanics, southeastern Australia—Evidence for upper mantle heterogeneity: *Contr. Mineral. Petrol.* **42,** 93–108.

Loughnan, F. C. (1969) *Chemical Weathering of the Silicate Minerals:* Elsevier, New York, 154 pp.

Norrish, K. (1968) Some phosphate minerals in soils: in *Trans. 9th Conf. Int. Soil Sci. Soc., Adelaide, Vol. 2,* J. W. Holmes, ed., Angus and Robertson, Sydney, Australia.

Norrish, K. and Chappell, B. W. (1977) X-ray fluorescence spectrography: in *Physical Methods in Determinative Mineralogy,* J. Zussman, ed., Academic Press, New York, 720 pp.

Wilson, R. E. (1978) Mineralogy, petrology and geochemistry of basalt weathering: B.Sc. thesis, Latrobe University, 55 pp.

(Received 12 November 1985; accepted 27 February 1987; Ms. 1530)